NASA TECHNICAL NOTE

NASA TN D-3391

NASA TN D-3391

TECHNIQUES FOR THE DESIGN, EVALUATION, AND ANALYSIS OF ENDLESS-LOOP TAPE TRANSPORTS FOR SATELLITE APPLICATIONS

by Kenneth W. Stark

Goddard Space Flight Center
Greenbelt, Md.

NATIONAL AERONAUTICS AND SPACE ADMINISTRATION • WASHINGTON, D. C. • MAY 1966

National Aeronautics And Space Administration

ERRATA

Technical Note D-3391

TECHNIQUES FOR THE DESIGN, EVALUATION, AND ANALYSIS OF ENDLESS-LOOP TAPE TRANSPORTS FOR SATELLITE APPLICATIONS

Kenneth W. Stark

May 1966

Replace page 22 of the subject paper with the attached page.

NASA-Langley, 1966

NASA TN D-3391

TECHNIQUES FOR THE DESIGN, EVALUATION, AND ANALYSIS OF ENDLESS-LOOP TAPE TRANSPORTS FOR SATELLITE APPLICATIONS

By Kenneth W. Stark

Goddard Space Flight Center
Greenbelt, Md.

NATIONAL AERONAUTICS AND SPACE ADMINISTRATION

For sale by the Clearinghouse for Federal Scientific and Technical Information
Springfield, Virginia 22151 – Price $2.00

ABSTRACT

The design of tape transports involves many areas of engineering. In order to obtain a design which provides optimum performance and survives the required environmental testing a careful design analysis must be made of critical areas such as velocity analysis, bearing preloading designs, stress analysis, rotational rates of bearing balls and races, tape cartridge designs, and system inertia and resonant characteristics. For designs where total life is an important criterion, it is seen that a compromise must be met between cartridge size and tape pack thickness because of the wear factor on tape. System resonant frequencies are analyzed and flutter and wow, power, and amplitude fluctuation measurements are performed and analyzed.

Disciplined design and testing approaches are advocated to ensure a reliable piece of equipment which will not be the cause of failure of any experiment or system.

CONTENTS

TECHNIQUES FOR THE DESIGN, EVALUATION, AND ANALYSIS OF ENDLESS-LOOP TAPE TRANSPORTS FOR SATELLITE APPLICATIONS*

by
Kenneth W. Stark
Goddard Space Flight Center

INTRODUCTION

Tape recorders are an essential part of any spacecraft instrumentation when data gathered by sensors must be stored until an orbit position has been reached where the spacecraft can be conveniently interrogated. Endless-loop tape recorders offer advantages over the two-reel systems primarily because multiple interrogations can be made without exceeding the required playback time to a ground station, tape-reversing mechanisms are not necessary, end-of-tape sensing devices are not required, momentum compensation is relatively simple, the single reel provides compact storage, and the tape velocity is in the same direction for both record and playback modes, minimizing errors due to tape skew and alignment.

The advent of interplanetary capsules and large satellites where considerable data must be stored necessitates large-capacity endless-loop tape recorders, in some cases recorders with capacities of 1200 or more feet of tape. In addition to size criteria, a rigid set of design specifications must be employed to assure a recorder with long life and reliability is obtained. Some of the main recorder components and their effects in related areas are analyzed in the present paper.

DESIGN CRITERIA

The performance requirements upon which the designs of endless-loop tape transports utilizing 1/2 inch wide tape containing 825 and 1200 feet lengths for use in endless-loop tape transports were based are as follows:

1. Flutter and wow: 0.8 percent peak-to-peak from 0 to 1000 cps.
2. Signal to noise ratio: 36 db.
3. Amplitude modulation: 4 to 8 percent peak-to-peak.
4. Mechanical power requirement: less than 2 watts at 0°C.

*This report was prepared previously as a thesis submitted to the Faculty of the School of Engineering and Architecture of The Catholic University of America in partial fulfillment of the requirements for the degree of Master of Aero-Space Engineering.

The recorder must meet the above specifications both before and after it is subjected to the following environmental tests:

1. Temperature tests at extremes of -5° and 55°C.
2. Vibration tests:
   a. Sinusoidal: 10 g (limit to 1/4-inch single amplitude), 5 to 2000 cps, 18-minute duration.
   b. Random: 20 g RMS, 20 to 2000 cps, 0.2 g^2/cps spectral density, 4-minute duration.

The basic endless-loop recorder consists of the following major components:

1. Tape reel.
2. Cover plate rollers.
3. Intermediate pulley or momentum flywheels.
4. Drive motor.
5. Pressure rollers.
6. Capstans.
7. Magnetic heads.
8. Endless-loop tape pack.
9. Tape support rollers.

In some cases, the same design principles and analyses apply to more than one of these components; the more difficult case is described herein when it can be applied to the less complex one as well. The capstans, the tape, the bearings, the system resonance characteristics, and the system inertial characteristics are covered in the present paper.

ANALYSIS OF RECORDER COMPONENTS AND SYSTEM CHARACTERISTICS

Capstans

As satellites become more sophisticated they incorporate numerous experiments involving the measurement of various parameters during the orbit. A recorder must be able to store this satellite information and to reproduce it without distortion when so required by a ground station. The capstans are among the most serious offenders of the many mechanical components which can cause distortion. Any variation in capstan circumferential speeds will change the velocity of the magnetic tape and introduce signal distortion commonly referred to as flutter and wow. Velocity differences caused by the capstan assembly can be attributed to radius runouts on the capstan shaft or on its associated pulleys, improper preloading methods, or damaged bearings.

Normally, when a flutter problem arises, a spectral analysis of the playback signal is made through a discriminator from which the periodic components are obtained. A velocity analysis

must be made to determine which mechanical components are responsible. In order to derive an equation which relates the various components which can affect the velocity of the tape and is based upon the usual condition of driving a capstan through one belt pass from a motor, one must have a fairly accurate knowledge of what contours the various diameters follow, e.g., whether they are elliptical, multiple nodes, or cam shaped. The equation can be expanded to cover the case where there is more than one reduction.

As a practical example, assume two circular machined diameters with an offset center of rotation (Figure 1); the symbols are defined in Appendix A:

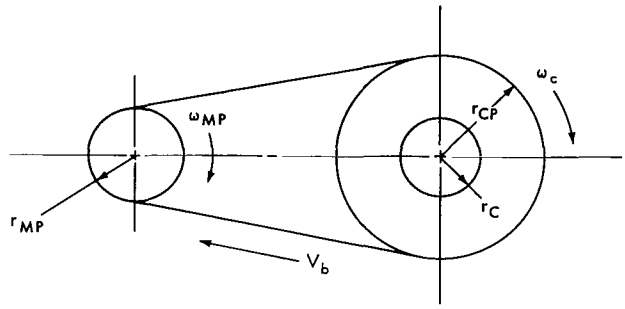

Figure 1—Circular machined diameters with an offset center of rotation.

$$V_b = r_{MP}\,\omega_{MP}$$

and

$$V_b = r_{CP}\,\omega_C \ ;$$

therefore,

$$\omega_C = \frac{V_b}{r_{CP}} = \frac{r_{MP}\,\omega_{MP}}{r_{CP}} \ .$$

But

$$V_C = r_C\,\omega_C \ .$$

Substituting for ω_C,

$$V_C = \frac{r_C\, r_{MP}\,\omega_{MP}}{r_{CP}} \ . \qquad (1)$$

Equation 1 expresses the tape velocity at the capstan V_C in terms of the radii and rotational rates. Now for the case where

$$\omega_{MP} = 835 \text{ rad/sec} \ ,$$

$$r_C = 0.250 \text{ in.} \ ,$$

$$r_{CP} = 1.00 \text{ in.} \ ,$$

and

$$r_{MP} = 0.16 \text{ in.} \ ,$$

$$V_C = \frac{(0.250)\,(0.16)\,(835)}{1.00} = 33.4 \text{ ips} \ .$$

However, if each pulley had a total indicated runout of 50×10^{-6} inches and all these tolerances coincided, the total percentage velocity change of the tape across the heads would be as follows:

$$\sum \frac{\Delta r}{r} \times 100 = 100 \left(\frac{0.000050}{0.250} + \frac{0.000050}{1.00} + \frac{0.000050}{0.16} \right)$$

$$= (0.000562)\ 100 = 0.056 \text{ percent peak-to-peak .}$$

This value of velocity deviation is usually well below that required as a specification. The flutter will have periodic components at 133 cps (motor) and 21 cps (capstan); the peak flutter will oscillate at 6.33 cps (beat frequency).

For more complicated radius contours (e.g., elliptical), the proper contour equation must be obtained and, from it, V_c must be obtained using the new radii expressions.

The velocity analysis of the ball bearing effects on tape velocity will be covered in another section; however, a direct factor which influences ball bearing performance will be discussed here.

The assembly that contains the capstan also contains the ball bearings which support the capstan Utilizing the duplex system of bearing preloading it is necessary to use end caps which contain the bearings in the capstan housing assembly. Proper design for the preloading technique must allow a few thousandths of an inch protrusion of the bearing race on each side of the housing to maintain the races under compression when mounted. It is essential, however, that the races are not so excessively compressed that distortion will result in the raceway and cause failure either in the raceway, balls, or both. (It is also important to note that the raceway thickness of a typical ball bearing for this use is approximately 0.023 inch.) Because of this important consideration, it was necessary to derive an equation which took into consideration the various physical parameters involved. In the derivation, one-half of the preloaded assembly is used and the other half is treated as the mirror image. The symbols used are defined in Appendix A and a schematic of the typical cross-sectional view of an end cap retaining the outer race of the ball bearing is shown in Figure 2.

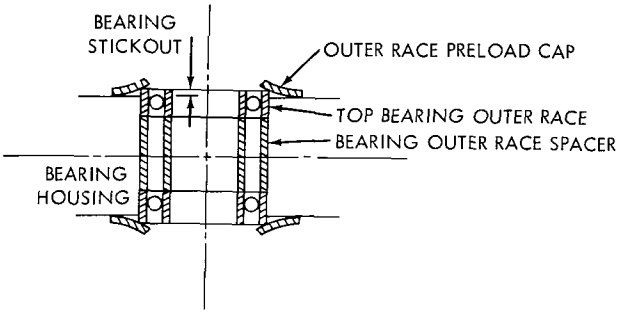

Figure 2—Schematic representation of typical cross section of an end cap.

The following equations are obtained (Reference 1):

$$E = \frac{S}{\epsilon} = \frac{SL}{\Delta L} ,$$

or

$$E\Delta L = SL(\text{for spacers and races}) ;$$

substituting,

$$E_1 \Delta L_1 = S_1 L_1$$

and

$$E_2 \Delta L_2 = S_2 L_2 ;$$

also,

$$\delta - (\Delta L_1 + \Delta L_2) = \Delta L_3 ,$$

$$S = \frac{P}{A} \text{ (for spacers and races)} ,$$

$$P = A_1 S_1 = A_2 S_2 ,$$

and

$$\Delta L_{3_{max}} = \frac{3P(m^2 - 1)}{4\pi m^2 E_3 L_3^3} \left[a^2 - b^2 + \frac{2m b^2 (a^2 - b^2) - 8m a^2 b^2 \ln \frac{a}{b} + 4a^2 b^2 (m+1)^2 \left(\ln \frac{a}{b}\right)^2}{a^2 (m-1) + b^2 (m+1)} \right] ;$$

$$\text{Let } X = \left[a^2 - b^2 + \frac{2m b^2 (a^2 - b^2) - 8m a^2 b^2 \ln \frac{a}{b} + 4a^2 b^2 (m+1)^2 \left(\ln \frac{a}{b}\right)^2}{a^2 (m-1) + b^2 (m+1)} \right] ,$$

then

$$\Delta L_3 = \frac{3P(m^2 - 1)}{4\pi m^2 E_3 L_3^3} X .$$

$$S_{3_{max}} = \frac{3P}{2\pi L_3^2} \left[1 - \frac{2m b^2 - 2b^2 (m+1) \ln \frac{a}{b}}{a^2 (m-1) + b^2 (m+1)} \right] ;$$

$$\text{Let } Y = \left[1 - \frac{2m b^2 - 2b^2 (m+1) \ln \frac{a}{b}}{a^2 (m-1) + b^2 (m+1)} \right] ,$$

then

$$S_3 = \frac{3P}{2\pi L_3^2} Y .$$

We now have seven unknowns (ΔL_1, S_1, ΔL_2, S_2, ΔL_3, P, and S_3) and seven equations which can be solved. Solving for ΔL_3,

$$\Delta L_3 = \frac{3\delta (m^2 - 1) X}{\left[\frac{Z L_1}{A_1 E_1} + \frac{Z L_2}{A_2 E_2} + 3X(m^2 - 1) \right]} \qquad (2)$$

where

$$Z = 4\pi m^2 E_3 L^3_3 .$$

Equation 2 will be used as an illustrative example by analyzing an existing condition. Values will also be found for P, S_1, S_2, S_3, ΔL_1, and ΔL_2.

Using the mirror-image concept, the amount of bearing outer race stickout on the 1200- and 825-foot recorder capstan assembly is 0.002 inch on one side. The values of the constants are

$$L_1 = 0.1562 \text{ in.} ,$$

$$L_2 = 0.346 \text{ in.} ,$$

$$m = \frac{1}{V} \times \frac{1}{0.3} = 3.33 ,$$

$$\delta = 0.002 \text{ in. (unloaded bearing stickout on one side)} ,$$

$$E_3 = 30 \times 10^6 \text{ psi} ,$$

$$L_3 = 0.062 \text{ in.} ,$$

$$a = 0.375 \text{ in.} ,$$

$$b = 0.225 \text{ in.} ,$$

$$E_1 = 30 \times 10^6 \text{ psi} ,$$

$$E_2 = 30 \times 10^6 \text{ psi} ,$$

$$A_1 = 0.0314 \text{ in}^2 ,$$

and

$$A_2 = 0.0314 \text{ in}^2$$

Using Equation 2 and substituting the given values for the constants result in

$$\Delta L_3 = 0.0017 \text{ in.}$$

The next step is to get the load on the edges P; from

$$\Delta L_3 = \frac{3P(m^2 - 1)}{4\pi m^2 E_3 L_3^3} X$$

we find

$$P = 540 \text{ lb.}$$

Then values for S_1 and S_2 are obtained:

$$S_1 = \frac{P}{A_1} = 17,200 \text{ psi}$$

and

$$S_2 = \frac{P}{A_2} = 17,200 \text{ psi.}$$

S_3 is obtained from

$$S_3 = \frac{3P}{2\pi L_3^2} Y$$

and by substituting the appropriate values is found to be

$$S_3 = 53,000 \text{ psi.}$$

The deflections of the bearing outer race and spacer are obtained as follows:

$$\Delta L_1 = \frac{S_1 L_1}{E_1} ,$$

$$\Delta L_1 = 0.0000893 \text{ in.} ,$$

and

$$\Delta L_2 = \frac{S_2 L_2}{E_2} ,$$

$$\Delta L_2 = 0.0001983 \text{ in.} ,$$

and, as found previously,

$$\Delta L_3 = 0.0017 \text{ in.}$$

Bearings

As previously mentioned, it is important that bearings, when supporting a load, be preloaded (Reference 2); that is, the bearings must be confined so that under no anticipated loading of the bearing assembly will a permanent deformation in the balls or raceway result. In the instrumentation field, as applied to space satellites, the anticipated loading is caused by temperature differences and random and sinusoidal vibration testing. Sinusoidal vibrations are usually the more critical of the test requirements because at resonant frequencies high amplification factors are observed which result in very high loads on the bearings.

Some factors other than improper preloading which can lead to bearing failure are lubricant failure, impurities mixed with the lubricant, lack of enough lubricant, excessive bearing speeds, improper bearing alignment, and improper bearing fits. These will not be discussed in this report as each is an extensive subject in itself.

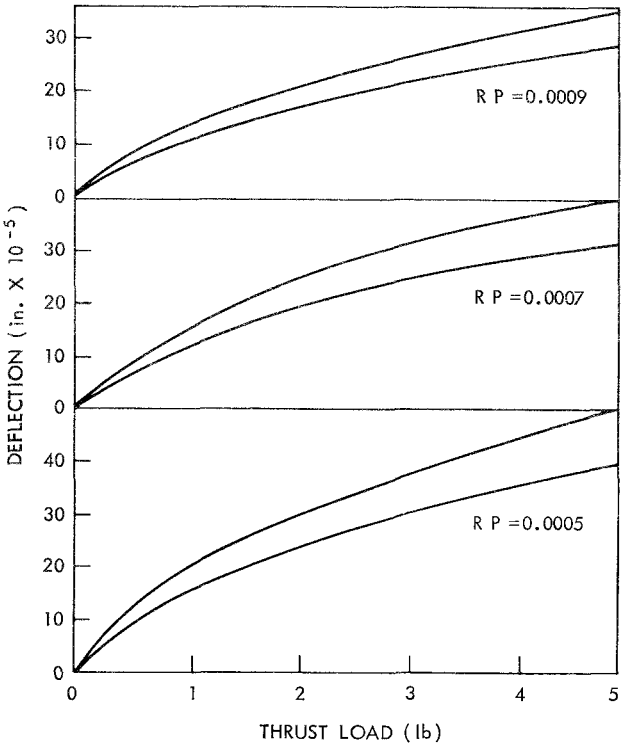

Figure 3—Ball bearing load-deflection curves; the two curves for each radial play (RP) value represent range of axial deflection as determined by manufacturing tolerance of raceway curvature.

There are essentially two methods of obtaining preloads on bearings; one is preloading by fixed distances, normally referred to as duplexing, and the other is preloading by loading, which is normally done with springs. In the case of the tape recorder, where precision runouts and alignment are required, the method normally used is that of duplexing. With this technique the load is applied to the bearing by machining a given amount off the face of either the inner or outer races. The amount machined off is determined from a load deflection curve of the bearing in question. Typical curves for the R2-6 bearing are shown in Figure 3. The reason for this type of preloading is that under no anticipated external loading will the bearing become unpreloaded; if it became unpreloaded there would be bouncing of the balls on the raceway resulting in high impact stresses and ultimate failure due to brinelling of the balls or raceways.

A sample calculation utilizing the R2-6 bearing and its load deflection curve will illustrate how the preload is determined. Let us use two R2-6 bearings with 0.0007-inch radial play

(Figure 4); the weight of the assembly times 20 g is 5.75 pounds.

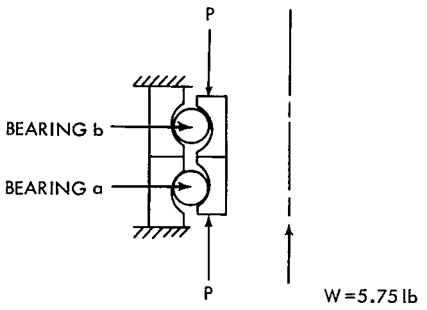

Figure 4—Preloaded R2-6 bearings.

First trial:

Deflection of each bearing δ_B under preload P = 2 lb:

Bearing a: $\delta_B = 21 \times 10^{-5}$ in.;
Bearing b: $\delta_B = 21 \times 10^{-5}$ in.

Deflection of one bearing with P + W = 7.75 lb:

Bearing a: $\delta_B = 44 \times 10^{-5}$ in.

Therefore bearing b is moved back by $(44-21)\times10^{-5}$ in. $= 23\times10^{-5}$ in. and becomes unpreloaded by 2×10^{-5} in.

This value of P is not sufficient; therefore P must be increased.

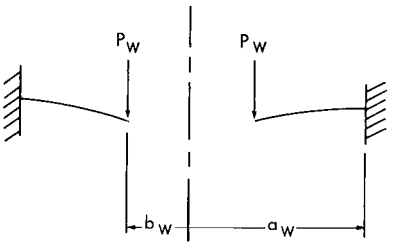

Figure 5—Preloaded Bellville spring washer.

Second trial:

Deflection of each bearing under P = 2.5 lb:

Bearing a: $\delta_B = 24 \times 10^{-5}$ in.;
Bearing b: $\delta_B = 24 \times 10^{-5}$ in.

Deflection of one bearing with P + W = 8.25 lb:

Bearing a: $\delta_B = 46 \times 10^{-5}$ in.

Therefore bearing b is moved back by 22×10^{-5} in. and is still preloaded by 2×10^{-5} in.

This value of P is sufficient.

In the case where precision runouts and alignment are not of prime importance spring preloading can be utilized. The advantage of this technique is that precision grinding of the races and the accurately bored holes required in duplexing are not necessary; the disadvantage is that, in the case of sinusoidal vibrations, a resonance may be excited in the spring mass system and may cause brinelling of the bearing. The preloading can be applied using Bellville spring washers or ordinary coil springs (Figure 5).

A sample calculation will illustrate the method of determining a Bellville spring washer preload for the hysteresis synchronous motor used in the tape recorder. Here (see Appendix A for definitions of symbols):

$$m = \frac{1}{0.3} = 3.3 ,$$

$$E = 17 \times 10^6 \text{ psi} ,$$

Weight of motor armature = 1 oz. ,

a_W = 0.3 in. ,

b_W = 0.14 in. ,

Number of g's = 20 ,

and

Resonant frequency desired = 1000 cps .

Find spring constant k, washer thickness t_w, and thrust and radial bearing loads T and R:

$$\omega_M = \frac{1}{2\pi}\sqrt{\frac{12k}{M}} ;$$

$$1000(2\pi) = \sqrt{\frac{12k(32.2)(16)}{1}} ;$$

and

$$k = 0.0638 \times 10^5 = 6380 \text{ lb/in.}$$

Next we must determine the washer thickness under 20 g's:

$$Y_{MAX} = \frac{3P_W(m^2-1)}{4\pi m^2 E t_W^3}\left[a_W^2 - b_W^2 + \frac{2m b_W^2 (a_W^2 - b_W^2) - 8m a_W^2 b_W^2 \ln\frac{a_W}{b_W} + 4a_W^2 b_W^2 (m+1)\left(\ln\frac{a_W}{b_W}\right)^2}{a_W^2(m-1) + b_W^2(m+1)}\right]$$

Substituting the appropriate values we obtain

$$Y_{MAX} = \frac{3P_W(m^2-1)}{4\pi m^2 E t_W^3}(0.0405) ,$$

but

$$\frac{Y_{MAX}}{P_W} = \frac{1}{k} = \frac{1}{6380} = 0.000157 \text{ in./lb.}$$

Using this value for Y_{MAX}/P_w and solving for the washer thickness,

$$t_w = 0.0149 \text{ in.}$$

To get a 1-pound load on the bearings for this value of t_w, the washer would have to be deflected 1/k or 0.000157 inch. If the spring went into resonance and obtained a Q of 10 at 20 g's the resultant linear displacement would be (at 1000 cps):

$$0.0035 \text{ inch - double amplitude}$$

or

$$0.00175 \text{ inch - single amplitude .}$$

Therefore, to keep the spring from unloading, the spring would have to have an initial deflection of 0.00175 inch. This results in

$$\frac{0.00175 \text{ in.}}{0.000157 \text{ in./lb}} \text{ or a } 11.1 \text{ lb load}$$

on the bearing which results in about 0.001 inch deflection on an R3 bearing.

An R-3 bearing has a contact angle of about 14°. Therefore, the radial load on the bearing for this angle is

$$R = \frac{T}{\tan \beta} = \frac{11.1}{\tan 14^\circ} = 44.6 \text{ lb.}$$

If, as mentioned in the section on capstans, there is a flutter and wow problem in the tape recorder and analysis doesn't show it to be any particular pulley, shaft, or rotating component defect, then the ball bearings must be analyzed. A derivation of the frequency of a point on a ball with respect to the races of the ball bearing with outer race fixed (Figure 6) follows. Here

ω_B = Frequency of point C on ball = $\frac{\theta}{t}$,

ω_m = Ball frequency about axis of bearing = $\frac{\alpha}{t}$,

ω_i = Inner race frequency ,

d_B = Ball diameter ,

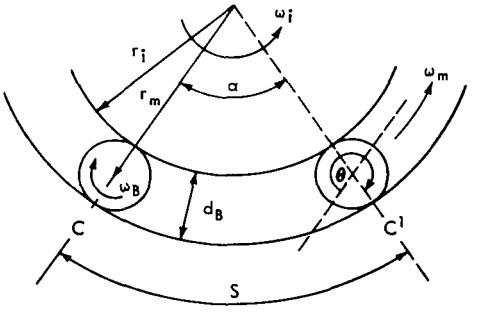

Figure 6—Schematic diagram showing ball bearings and inner and outer races.

$$V = r_i \omega_i ,$$

$$V_m = \frac{V}{2} = \frac{r_i \omega_i}{2} = r_m \omega_m ,$$

and

$$\omega_m = \frac{r_i \omega_i}{2r_m} .$$

Now

$$S = \alpha \left(r_m + \frac{d_B}{2} \right) = \theta \frac{d_B}{2} ,$$

$$\frac{\alpha}{t} \left(r_m + \frac{d_B}{2} \right) = \frac{\theta}{t} \frac{d_B}{2} ,$$

and

$$\omega_m \left(r_m + \frac{d_B}{2} \right) = \omega_B \frac{d_B}{2} ,$$

resulting in

$$\omega_B = \omega_m \left(\frac{2r_m + d_B}{d_B} \right)$$

Substituting for ω_m we obtain

$$\omega_B = \frac{r_i \omega_i}{2r_m} \left(\frac{2r_m + d_B}{d_B} \right)$$

and

$$\omega_B' = \frac{r_i \omega_i}{r_m} \left(\frac{2r_m + d_B}{d_B} \right) \qquad (3)$$

Equation 3 is multiplied by two because the ball touches the inner race also.

A derivation of the case with inner race fixed follows. The same figure and symbols used for the preceding example hold except

$$r_o = \text{Radius of outer race}$$

$$\omega_o = \text{Outer race frequency} .$$

Here

$$S = \alpha r_o = \theta \frac{d_B}{2} ,$$

$$\frac{\alpha}{t} r_o = \frac{\theta}{t} \frac{d_B}{2} ,$$

and

$$\omega_m r_o = \omega_B \frac{d_B}{2} ,$$

resulting in

$$\omega_B = \frac{2\omega_m r_o}{d_B} .$$

Substituting for ω_m results in

$$\omega_B = \frac{r_o^2 \omega_o}{d_B r_m}$$

and

$$\omega_{B'} = \frac{2r_o^2 \omega_o}{d_B r_m} \qquad (4)$$

where the factor 2 accounts for the ball hitting the inner race also.

Tape

A three-year study of the recorder design using a 1200-foot endless-loop tape has revealed more problems with tape reliability than with any other part of the system. Some typical problems are:

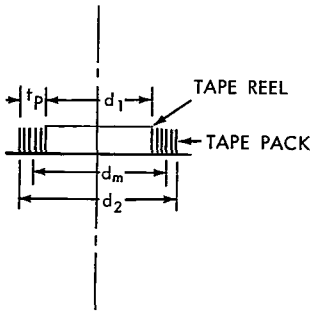

(a) Tape cartridge.

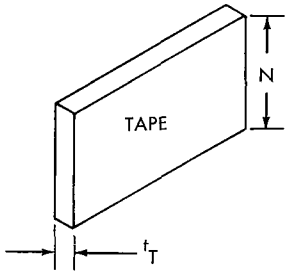

(b) Tape reel.

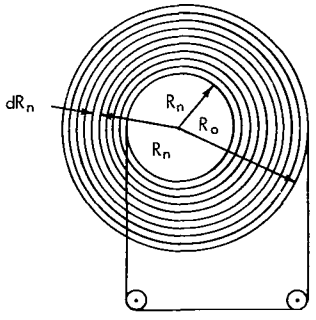

(c) Tape pack.

Figure 7—Configuration of tape cartridge, tape reel, and tape pack.

1. Excessive wear on both the lubricated and oxide coated sides of the tape so that the required operational lifetime of the recorder is seriously jeopardized.
2. Excessive shrinkage of the tape at the required test temperature of 60°C, causing the endless loop to become tight and to jam.
3. Variations in magnetic properties between tape samples causing problems in electronic circuit design for the record and playback amplifiers.
4. Variations in oxide wear between samples causing an unpredictable decay rate of tape performance.
5. Variations in coefficient of friction of the tape surfaces sufficient to cause variations in internal power dissipation of the tape back.

Although these problems have been brought to the attention of industry, not much progress has been made in solving them because of their complexity. In the meantime it has been necessary to optimize the cartridge design and the size of the endless loop tape pack so that we can use the tape presently available. To this end certain equations which correlate various physical parameters of the tape such as reel diameter d_1, pack thickness t_p, tape layer width N, tape length L, tape thickness t_T, and mean tape pack diameter d_m were derived and are given below for a cartridge of the basic configuration shown in Figure 7 (see Appendix B for the operational discussion):

$$d_m = d_1 + t_P \,, \tag{5}$$

$$L = \pi d_m \frac{t_P}{t_T} \,, \tag{6}$$

and

$$A = 2\pi N d_m \left(\frac{t_P}{t_T} - 1\right) \,, \tag{7}$$

With these three equations a tape cartridge size can be obtained for any given tape requirements; the cartridge reel size will vary for different tape lengths. Normally, a tape pack thickness of about 0.8 inch has been found satisfactory for our use. The following example shows the application of the three equations to the 825-foot cartridge; the design values are

$$t_P = 0.7 \text{ in.},$$

$$L = 825 \text{ feet or } 9900 \text{ in.},$$

$$t_T = 0.0012 \text{ in. for MT 22049 tape},$$

and

$$N = 0.5 \text{ in.}$$

Substituting,

$$d_m = \frac{t_T L}{\pi t_P} = \frac{0.0012(9900)}{3.14(0.7)} = 5.40 \text{ in.},$$

$$d_1 = d_m - t_P = 4.70 \text{ in.},$$

and

$$A_{825'} = 2\pi N\left(\frac{L}{\pi} - d_m\right) = 3.14(3150 - 5.40) = 9900 \text{ sq in.};$$

for the 1200-foot cartridge

$$A_{1200'} = 3.14(4580 - 7.9) = 15,380 \text{ sq in.}$$

As can be seen, the tape contact area is reduced significantly by reducing tape length.

Recently we have been conducting experiments with compact versions of the large 1/2-inch by 1200-foot recorders used in the Nimbus Satellite sensory ring module to determine the effect of increased pack thickness on tape wear, life, and general performance characteristics. It can be seen that as reel diameter d_1 is reduced tape pack thickness t_P is increased for a given length of tape; this could affect overall tape life (mechanical and electrical), energy dissipation, performance characteristics, and overall power. A derivation of the kinetic energy necessary to move the tape pack shows that this energy does not depend upon pack thickness but rather on the tape length and linear tape velocity. The kinetic energy can be calculated as shown below, (for convenience of calculation, it is assumed that the pack consists of a series of concentric circles (Figure 7(c)):

$$dI = dMR_n^2 = \frac{2\pi R_n N dR_n \rho R_n^2}{g}.$$

Substituting

$$k_T = \frac{2\pi N\rho}{g},$$

$$dI = k_T R_n^3 dR_n.$$

Now

$$dT_e = \frac{1}{2} dI \omega_n^2 ,$$

where $\omega_n^2 = V_C^2/R_n^2$. Substituting,

$$dT_e = \frac{1}{2} k_T V_C^2 \left(\frac{R_n^3}{R_n^2} dR_n \right)$$

and

$$T_e = \frac{1}{2} k_T V_C^2 \int_{R_r}^{R_0} R_n \, dR_n = \frac{1}{4} k_T V_C^2 (R_0^2 - R_r^2) = \frac{1}{4} k_T V_C^2 (R_0 - R_r)(R_0 + R_r)$$

$$= \frac{1}{4} k_T V_C^2 (t_P)(d_m) = \frac{1}{4} k_T V_C^2 t_P \left(\frac{Lt_T}{\pi t_P} \right) = \frac{\rho L t_T N V_C^2}{2g}$$

Let

$$C = \frac{\rho t_T N}{2g} ;$$

then, for a given tape size,

$$T_e = CLV_C^2 . \tag{8}$$

The next step is to determine if the contact area between layers of tape increases appreciably as the pack thickness increases for a given length of tape; an appreciable increase would possibly increase the power required to drive the cartridge and significantly increase the tape wear, thereby seriously reducing the total life of the tape.

Combining Equations (6) and (7) we get

$$A = 2N(L - \pi d_m) . \tag{9}$$

Equation (9) shows that for a long tape (e.g., 1200 feet long) the total surface area, for a constant tape length, will not vary significantly as the mean pack diameter becomes smaller. (It should be noted here that the maximum reasonable mean pack diameter is about 8 inches and the minimum is

about 3 inches.) As a result, the power and wear associated with this increased contact area, for constant values of L, will not add considerably to that due to the larger interlayer $(\Delta\omega_n)$ (see Appendix C).

The study of entrance and exit tensions (Reference 10) caused by an increase in pack thickness might be more significant. Figures 8 and 9 and Table 1 show how those tensions vary for different tape speeds and temperatures. The power P_P required to drive the tape pack is a function of the exit and entrance tensions T_1 and T_2 and the tape speed V_C:

$$P_P = 7.08 \times 10^{-3} F' V_C \qquad (10)$$

where F' is the difference between T_1 and T_2 in ounces and P_P is measured in watts.

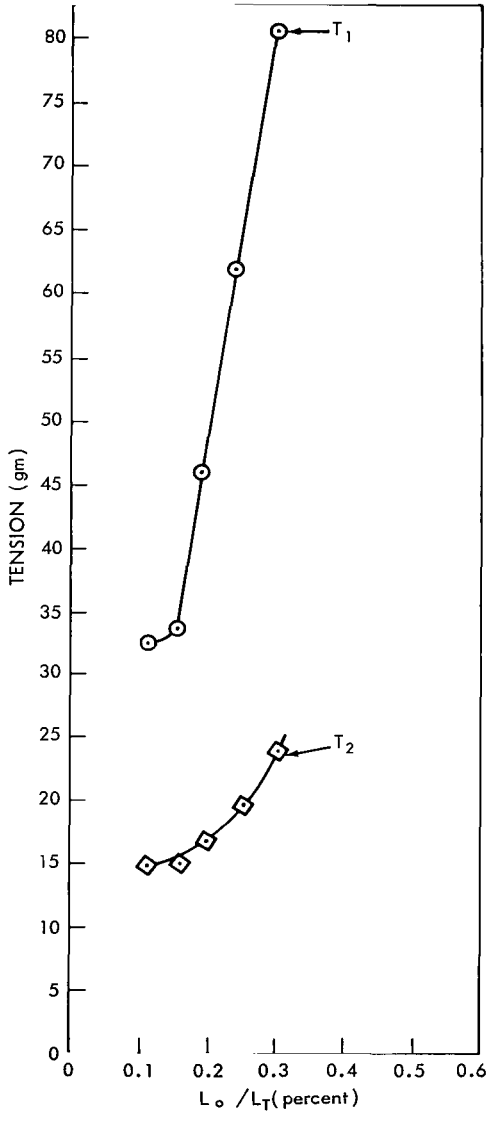

Figure 8—L_O/L_T against tension for 1200-foot-long tape at a tape speed of 0.4 inch per second. Run 1-1; temperature, 78°F; relative humidity, 60 percent. L_O, normal operating loop length; L_T, total tape length.

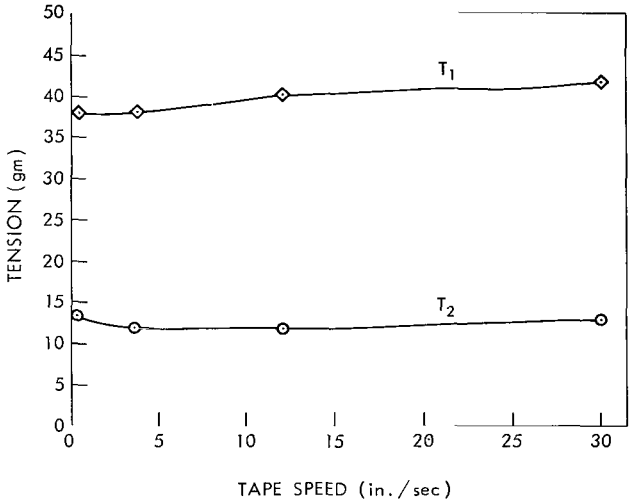

(a) Run 14-5; temperature, 121°F; relative humidity, 47 percent.

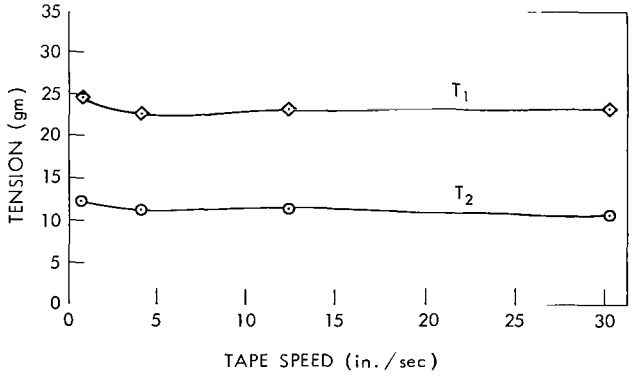

(b) Run 2-5; temperature, 75°F; relative humidity, 58 percent.

Figure 9—Tape speed against tape tension for 1200-foot-long tape with 1.33-foot-long normal operating loop.

System Resonance Characteristics

A tape recorder drive system consists of inertial masses (e.g., flywheel, pulleys, capstans, bearings, and tape) and connecting links that have spring constants and damping coefficients (e.g., polyester film belts (Reference 3), magnetic tape, oil, and motors). In any one recorder design, these combinations form a torsional spring, damping, and inertial mass system (Reference 4) with a number of natural frequencies associated with it. It is important to know what these frequencies are for the following two reasons:

1. There must not be a natural frequency of any system close to any impressed frequency in the recorder (e.g., in the motor, pulleys, or bearings) which will be able to excite the natural frequencies into resonance and so produce excessive signal distortion in the information recorded on the tape.

2. If during testing of the recorder a periodic flutter component is found which exceeds the required specifications and no rotating mechanical component can be found to be contributing to it, then the natural frequencies of the system must be investigated.

Table 1

Exit and Takeup Tension Levels for Normal Operating Loop Length (Station 0) for 1200-Foot Roller-Type Cartridge.

	Tape speed (ips)	Exit tension T_1 (gm)	Takeup tension T_2 (gm)	$T_1 - T_2$ (gm)
Run 1 (78°F 1200')	0.4	25.5	11	14.5
	3.75	18	10	8
	12	18.5	6.5	12
	30	18.5	5.0	13.5
Run 3 (121°F 1200')	0.4	19.5	5.0	14.5
	3.75	17	9.0	8
	12	27	7.0	20
	30	9	3.5	5.5
Run 7 (78°F 750')	0.4	16.5	7.0	9.5
	3.75	15	6.0	9
	12	15	4.5	10.5
	30	14	4.0	10
Run 8 (42°F 750')	30	35	15	20
Run 9 (121°F 750')	0.4	35	16	19
	3.75	40	16.5	23.5
	12	35	18	17
	30	20	11	9
Run 10 (78°F 500')	0.4	22.5	11	11.5
	3.75	25	10.5	14.5
	12	27	9	18
	30	37	8	26
Run 12 (121°F 500')	0.4	29	15	14
	3.75	27.5	12	15.5
	12	22.5	10	12.5
	30	25	9	16

The technique which is used to determine the system natural frequencies by assuming a system consisting of a motor and two belt passes will be illustrated (Figure 10). For simplification, items such as the frictional drag of ball bearings, the damping factor of the oil in the bearings, and feedback tension pulsations from the tape pack will be omitted. The derivation will be based upon what happens when instantaneous stoppage of I_2 causes the two belts to stretch and then analyzing the equations of motion when I_2 is released again.

For pulley 0 (Figure 10(b)),

$$- I_0 \ddot{\theta}_0 + \tau(t) + k_M \theta_0 r_0 + C_M \dot{\theta}_0 r_0 - k_1 (r_0 \theta_0 - R_1 \theta_1) r_0 - C_1 (r_0 \dot{\theta}_0 - R_1 \dot{\theta}_1) r_0 = 0$$

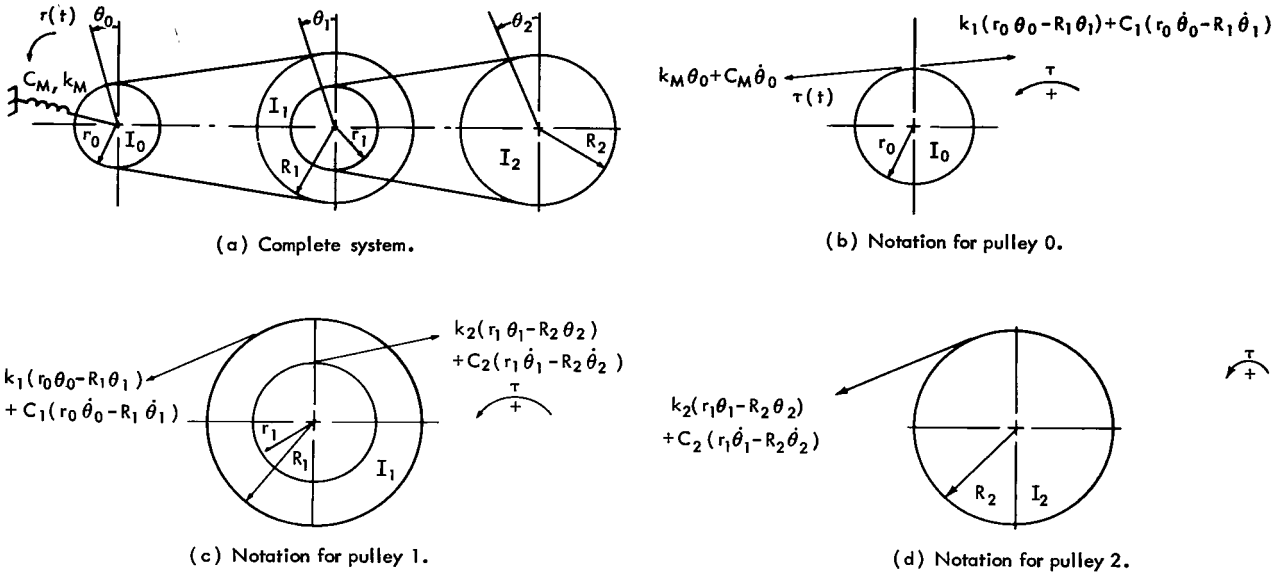

(a) Complete system.

(b) Notation for pulley 0.

(c) Notation for pulley 1.

(d) Notation for pulley 2.

Figure 10—System of a motor and two belt passes.

reduces to

$$I_0 \ddot{\theta}_0 + \left(C_1 r_0^2 - C_M r_0\right) \dot{\theta}_0 - C_1 R_1 r_0 \dot{\theta}_1 + \left(k_1 r_0^2 - k_M r_0\right) \theta_0 - k_1 R_1 r_0 \theta_1 = \tau(t),$$

resulting in

$$\ddot{\theta}_0 + M_1 \dot{\theta}_0 + M_2 \dot{\theta}_1 + M_3 \theta_0 + M_4 \theta_1 = M_5 \tag{11}$$

where

$$M_1 = \frac{C_1 r_0^2 - C_M r_0}{I_0},$$

$$M_2 = -\frac{C_1 R_1 r_0}{I_0},$$

$$M_3 = \frac{k_1 r_0^2 - k_M r_0}{I_0},$$

$$M_4 = -\frac{k_1 R_1 r_0}{I_0},$$

and

$$M_5 = \frac{\tau(t)}{I_0}.$$

For pulley 1 (Figure 10(c)),

$$-I_1\ddot{\theta}_1 + k_1\left(r_0\theta_0 - R_1\theta_1\right)R_1 + C_1\left(r_0\dot{\theta}_0 - R_1\dot{\theta}_1\right)R_1 - k_2\left(r_1\theta_1 - R_2\theta_2\right)r_1 - C_2\left(r_1\dot{\theta}_1 - R_2\dot{\theta}_2\right)r_1 = 0$$

reduces to

$$I_1\ddot{\theta}_1 + \left(C_1R_1^2 + C_2r_1^2\right)\dot{\theta}_1 - C_2R_2r_1\dot{\theta}_2 + \left(k_1R_1^2 + k_2r_1^2\right)\theta_1 - k_2R_2r_1\theta_2 - C_1r_0R_1\dot{\theta}_0 - k_1r_0R_1\theta_0 = 0\ ,$$

resulting in

$$\ddot{\theta}_1 + M_6\dot{\theta}_1 + M_7\dot{\theta}_2 + M_8\dot{\theta}_0 + M_9\theta_1 + M_{10}\theta_0 + M_{11}\theta_2 = 0 \qquad (12)$$

where

$$M_6 = \frac{C_1R_1^2 + C_2r_1^2}{I_1}\ ,$$

$$M_7 = -\frac{C_2R_2r_1}{I_1}\ ,$$

$$M_8 = -\frac{C_1r_0R_1}{I_1}\ ,$$

$$M_9 = \frac{k_1R_1^2 + k_2r_1^2}{I_1}\ ,$$

$$M_{10} = -\frac{k_1r_0R_1}{I_1}\ ,$$

and

$$M_{11} = -\frac{k_2R_2r_1}{I_1}\ .$$

For pulley 2 (Figure 10(d)),

$$-I_2\ddot{\theta}_2 + k_2\left(r_1\theta_1 - R_2\theta_2\right)R_2 + C_2\left(r_1\dot{\theta}_1 - R_2\dot{\theta}_2\right)R_2 = 0$$

reduces to

$$I_2\ddot{\theta}_2 + C_2R_2^2\dot{\theta}_2 - C_2r_1R_2\dot{\theta}_1 + k_2R_2^2\theta_2 - k_2r_1R_2\theta_1 = 0\ ,$$

resulting in

$$\ddot{\theta}_2 + M_{12}\,\dot{\theta}_2 + M_{13}\,\dot{\theta}_1 + M_{14}\,\theta_2 + M_{15}\,\theta_1 = 0 \tag{13}$$

where

$$M_{12} = \frac{C_2 R_2^2}{I_2} ,$$

$$M_{13} = -\frac{C_2 r_1 R_2}{I_2} ,$$

$$M_{14} = \frac{k_2 R_2^2}{I_2} ,$$

and

$$M_{15} = -\frac{k_2 r_1 R_2}{I_2} .$$

It should be noted here that, in order to solve these equations, it is necessary to know C_M, k_M, C_1, C_2, k_1, k_2, and $\tau(t)$. Also, in reality, the factors that are neglected for this example must be known in order to get a valid answer. Many of these factors either are not known or are peculiar to the particular recorder used which means that much preliminary testing and research is necessary to determine needed coefficients.

The following example applies these equations to obtain the natural frequency of a single belt system utilizing I_0 and I_1 of the first belt pass. This example is based upon the motor and pully delivering a constant torque to the system. The motor is assumed as the base (i.e., θ_0 rotates with the motor and its pulley).

Therefore, $\theta_0 = \dot{\theta}_0 = \ddot{\theta}_0 = 0$ and also, for this example, C_1 is assumed to equal 0.

To solve for the natural frequency of I_1, Equation (12) is used. However, from the previous assumptions

$$\theta_0 = \dot{\theta}_0 = 0 ,$$

$$\dot{\theta}_2 = \theta_2 = 0 \qquad \text{(no pulley)} ,$$

and

$$M_6 = M_7 = M_8 = M_{11} = 0 ,$$

resulting in

$$\ddot{\theta}_1 + M_9 \theta_1 = 0 \tag{14}$$

where

$$M_9 = \frac{k_1 R_1^2}{I_1}$$

and

$$k_1 = 27 \text{ lb/in.} ,$$

$$R_1 = 1.00 \text{ in.} ,$$

$$I_1 = 1.12 \times 10^{-4} \text{ lb in. sec}^2 .$$

Equation (14) is a homogeneous second order differential equation; substituting a solution of the form

$$\theta_1 = Ke^{\phi t} ,$$

$$\dot{\theta}_1 = K\phi e^{\phi t} ,$$

and

$$\ddot{\theta}_1 = K\phi^2 e^{\phi t}$$

into Equation (14),

$$K\phi^2 e^{\phi t} + M_9 Ke^{\phi t} = 0$$

or

$$\left(\phi^2 + M_9\right) Ke^{\phi t} = 0 .$$

Here

$$\phi^2 = -M_9$$

or

$$\phi_{1,2} = \sqrt{-M_9} = \lambda_{1,2} + i\omega_{1,2} ,$$

where $\lambda_{1,2}$ are the damping rates of arms $K_{1,2}$ and $\omega_{1,2}$ are the rotating frequencies of $K_{1,2}$, resulting in

$$\theta_1 = K_1 e^{\phi_1 t} + K_2 e^{\phi_2 t}$$

Since there is no damping in this example, $\lambda_{1,2} = 0$, resulting in

$$i\omega_{1,2} = i\sqrt{M_9}$$

or

$$\omega_{1,2} = \sqrt{M_9}$$

where

$$M_9 = \frac{k_1 R_1^2}{I_1} = \frac{(27)(1)^2}{1.12 \times 10^{-4}} = 24.1 \times 10^4$$

and

$$f_N = \frac{1}{2\pi}\sqrt{24.1 \times 10^4} = 78.7 \text{ cps} .$$

System Inertial Characteristics

In the initial design of a recorder system it is often very important to determine the starting torque required to accelerate the system up to speed in a given time. This torque determines the instantaneous power required and so enables proper circuit designs to be made.

An example of how reflected inertias are determined for a pulley system follows. A diagram of the pulley system is given in Figure 10(a). The inertia will be reflected back to the driving motor. Let

$$\tau_R = \tau_0' + \tau_1' + \tau_2' ,$$

where τ_R is the total reflected torque at pulley 0 and τ_0', τ_1', and τ_2' are the torques of the respective pulleys as seen at pulley 0. The inertial torques of the respective pulleys are τ_0, τ_1, and τ_2

where

$$\tau_0 = I_0 \ddot{\theta}_0 = F_0 r_0 = \tau_0'$$

and

$$F_0 = \frac{I_0 \ddot{\theta}_0}{r_0} ;$$

$$\tau_1 = I_1 \ddot{\theta}_1 = F_1 R_1$$

and

$$F_1 = \frac{I_1 \ddot{\theta}_1}{R_1} ,$$

but

$$F_1 = F_0 ;$$

and

$$\tau_1' = F_1 r_0 = \frac{I_1 \ddot{\theta}_1 r_0}{R_1} ;$$

$$\tau_2 = I_2 \ddot{\theta}_2 = F_2 R_2$$

and

$$F_2 = \frac{I_2 \ddot{\theta}_2}{R_2} ,$$

but

$$F_2 = F_3$$

Therefore, the torque of pulley 2 as seen at pulley 1 is

$$F_3 r_1 = \frac{I_2 \ddot{\theta}_2 r_1}{R_2} = FR_1 ,$$

where F is the force seen on pulley 1 at radius R_1 due to the reflected torque from pulley 2.

$$F = \frac{I_2 \ddot{\theta}_2 r_1}{R_2 R_1} ,$$

and

$$\tau_2' = Fr_0 = \frac{I_2 \ddot{\theta}_2 r_1}{R_2 R_1} r_0 .$$

Therefore, since

$$\tau_R = \tau_0' + \tau_1' + \tau_2' ,$$

$$I_R \ddot{\theta}_0 = I_0 \ddot{\theta}_0 + \frac{I_1 \ddot{\theta}_1 r_0}{R_1} + \frac{I_2 \ddot{\theta}_2 r_1 r_0}{R_2 R_1} . \qquad (15)$$

Now

$$V_0 = V_1 ,$$

$$r_0 \dot{\theta}_0 = R_1 \dot{\theta}_1 ,$$

$$r_0 \ddot{\theta}_0 = R_1 \ddot{\theta}_1 ,$$

and

$$v_1 = V_2 ,$$

$$r_1 \dot{\theta}_1 = R_2 \dot{\theta}_2 ,$$

$$r_1 \ddot{\theta}_1 = R_2 \ddot{\theta}_2 .$$

Therefore,

$$\ddot{\theta}_1 = \frac{r_0 \ddot{\theta}_0}{R_1}$$

and

$$\ddot{\theta}_2 = \frac{r_1 \ddot{\theta}_1}{R_2} = \frac{r_1}{R_2}\left(\frac{r_0 \ddot{\theta}_0}{R_1}\right) = \frac{r_1 r_0 \ddot{\theta}_0}{R_2 R_1} .$$

Substituting these values into Equation 15 we get

$$I_R \ddot{\theta}_0 = I_0 \ddot{\theta}_0 + \frac{I_1 r_0}{R_1}\left(\frac{r_0 \ddot{\theta}_0}{R_1}\right) + \frac{I_2 r_1 r_0}{R_2 R_1}\left(\frac{r_1 r_0 \ddot{\theta}_0}{R_2 R_1}\right)$$

which becomes

$$I_R = I_0 + I_1\left(\frac{r_0}{R_1}\right)^2 + I_2\left(\frac{r_1 r_0}{R_2 R_1}\right)^2 . \qquad (16)$$

This method of analysis can be used for systems with any number of degrees of freedom.

ANALYSIS OF DESIGN TECHNIQUES

Flutter and Wow

In a tape transport, one of the most useful and efficient ways of proving the design and determining its performance is by measuring the flutter and wow (References 5 and 6).

Basically, the function of a tape recorder is to record data from a given source (e.g., experiments and various sensing transducers) and to store it until it is commanded by a ground station to play it back. When this information is received at the ground station it should be exactly as it was when recorded from the original source, but, unfortunately, this rarely happens in practice. The signal is usually distorted in frequency because of the variation in the linear velocity of the tape across the magnetic heads. This type of distortion is called flutter and wow. Wow is a term usually reserved for frequency distortion below 10 cps; flutter is used for frequencies above 10 cps and is generally the term used in instrumentation recording. The variation in the linear velocity across

the heads can be caused by factors such as radial runouts of mechanical rotating components, violin string effect as the tape crosses the magnetic heads, natural frequencies of the torsional vibration system set up by the motors, pulleys, and interconnecting polyester film belts, pulsations set up in the tape by the interlayer friction of the tape in the cartridge and ball-bearing noise.

The instruments shown in Figure 11 are used to determine the amount of flutter present and to analyze it to determine its origin. These instruments are used in the order shown in Figure 12. First, a signal is recorded onto the recorder for a full tape cycle and then played back through the playback amplifier. The signal from the amplifier is put through a bandpass filter to eliminate extraneous external noise pickup and any 60-cycle hum which has been picked up. It is then fed into a discriminator which converts any deviation from the signal recorded into a voltage output. This output is then passed through an output filter so that it can be separated into different frequency bands to try to isolate the particular frequencies which are causing the flutter. The output is then recorded onto a visicorder which shows the flutter frequency in a visible manner which can then be analyzed. A wave analyzer can also be used to determine the relative contribution of the various flutter components.

Once this has been done, two approaches are made to resolve the factors contributing to flutter.

1. All periodic flutter components found are compared with all mechanical and system resonant frequencies. Usually the main flutter sources are located and they can be eliminated or reduced to a level which is acceptable. The periodic flutter components caused by mechanical parts normally range from 0 to 150 cps. Resonant frequencies can range up to 700 cps or higher.

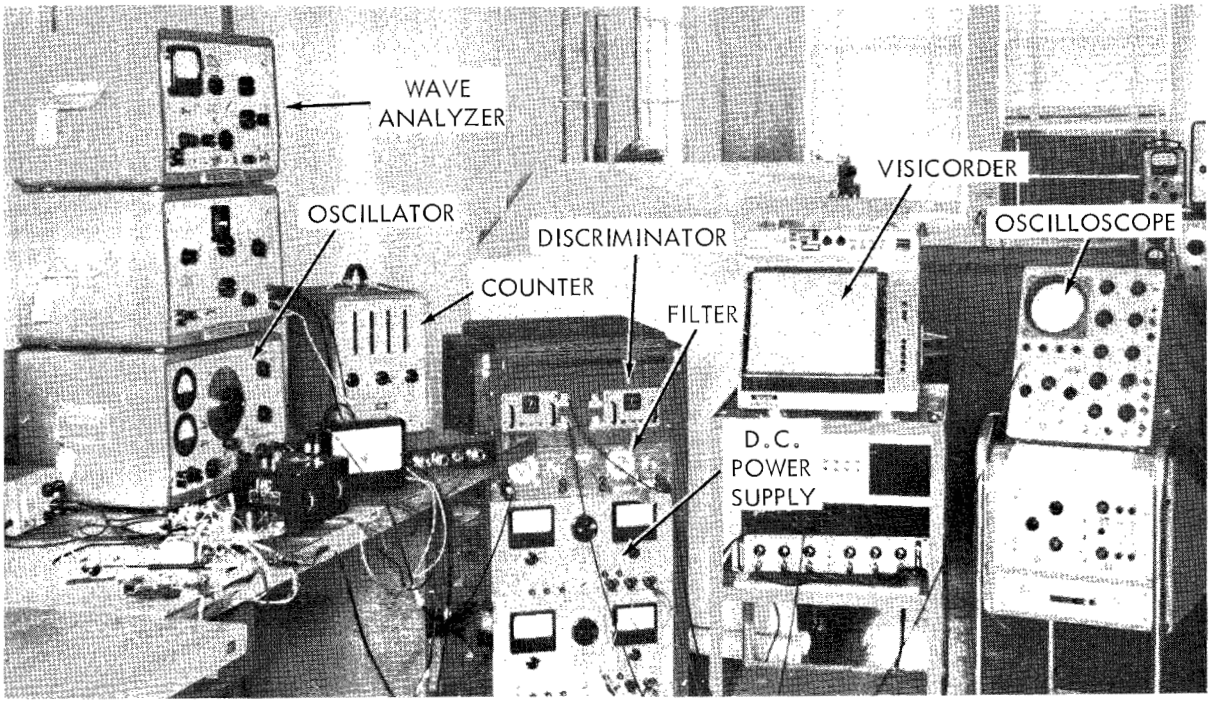

Figure 11—Flutter analysis equipment.

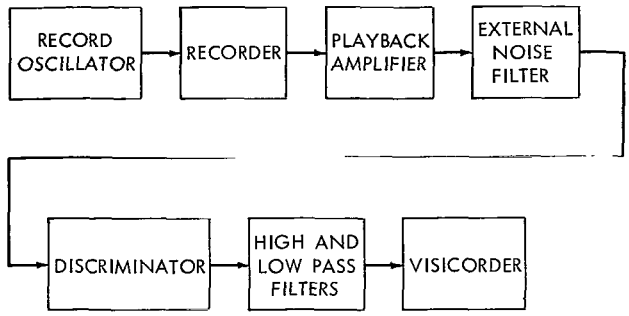

Figure 12—Schematic diagram of flutter analysis equipment.

2. Random flutter is that remaining after the periodic flutter has been separated from the total flutter. Sometimes the entire flutter spectrum is random; in this case the task of reducing or eliminating it becomes very difficult. One cause for this random flutter is the granular nature of the oxide particles on the tape which rub against the heads and cause a large number of very small impulse forces. Another cause is the random slip-stick phenomena which occur internally in the endless-loop cartridge and are caused by variations in the coefficients of friction and internal tensions. Compensating devices are used to reduce this flutter in the more sophisticated satellite where the allowable flutter is at a very low level. One of the more common techniques is to record a timing track from a very accurate clock (accuracy of 1 part in 10^6) on one channel of the tape. When played back to the ground station, this timing track, which is in error now by the amount of flutter, is corrected to read the proper frequency. This automatically corrects the information signals too.

Flutter is essentially measured in percent deviation rms or peak-to-peak over a particular bandwidth. Many manufacturers of tape recorders quote flutter in rms, but, unfortunately, this gives an erroneous concept of the true deviation. In order to determine the absolute deviation, which is the only deviation to use in analysis, the peak-to-peak deviation must be known. It is quite common to find a factor of 2.8 used for the conversion to peak-to-peak flutter, but this factor is correct only if the flutter component is a pure sine wave. When the waveform becomes a superposition of many sine waves or becomes completely random the factor is no longer 2.8.

As an example, let us assume that a recorder is found to have flutter which is completely random in nature with a normal (Gaussian) distribution where the flutter peaks exceed twice the standard deviation only 5 percent of the time. The standard deviation σ is also the rms value of flutter. Therefore, according to the Gaussian distribution shown in Figure 13,

$$4\sigma = \text{Peak-to-peak flutter}$$

and

$$\sigma = \text{rms value of flutter} = \frac{\text{Peak-to-peak flutter}}{4}$$

Another interesting approach is an analysis of the changes in the rms value of the random flutter with increasing flutter bandwidth. Available data in this area show that it is fairly reasonable to assume that the power spectral density D is uniform. The relationship between D, the

bandwidth B, and the standard deviation σ is

$$\sigma^2 = DB \, . \qquad (17)$$

The rms value is therefore equal to $\sqrt{DB}$. From this it can be seen that the random flutter increases with the bandwidth if D is constant.

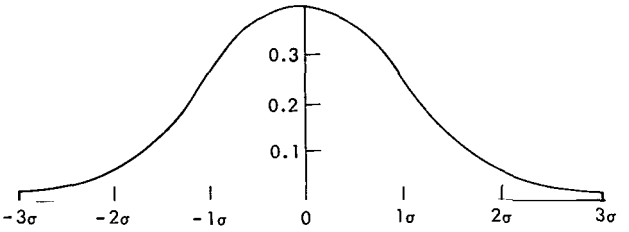

Figure 13—Normal Gaussian curve.

As an example, Figure 14 presents flutter traces of a 50-kc signal recorded and played back at 33 ips through an analysis system similar to that shown in Figure 11. Each flutter trace has the following calibration:

1. 20 millisec/cm sweep
2. 0.6 percent peak-to-peak flutter/cm

From these traces it is found that there are two distinct flutter components of 60 and 120 cps. Also, it is evident that the prediction of Equation 17 is correct; that is, as the bandwidth increases, the random flutter increases as shown in Table 2.

Table 2

Changes in Bandwidth and Flutter Shown in Figure 14.

Bandwidth (cps)	Random Flutter (percent peak-to-peak)
0 to 100	1.2
0 to 500	1.44
0 to 1000	1.44
0 to 2000	1.64
0 to 5000	1.92

Power Measurements

Performance can also be evaluated and analyzed by the measurement of the power required to operate the system and its characteristics. One of the two methods which can be used for this measurement utilizes a dc motor, and the other, a tensiometer.

The dc motor technique is used mainly to determine overall system power and individual component power by a process of elimination. To use this method the motor must be calibrated. In a dc motor the current is proportional to the torque output; as a result, a calibration curve can be obtained for the motor by using a small dynamometer and an ammeter. Once this calibration curve is obtained the motor is placed into the transport and power measurements are taken by both running the system with all components and removing the components one by one.

The tensiometer is a measuring device that enables a tension trace to be taken of the tape as it is running at various speeds. With this method we find not only the tension in the tape, and thus power, but also the wave shape of the tension. A typical trace is shown in Figure 15; it consists of a definite 120 cps component and a possible 17.9 cps component. As can be seen in Figure 15, the trace consists of both periodic and random components. This is valuable information when a particular complicated flutter problem is analyzed.

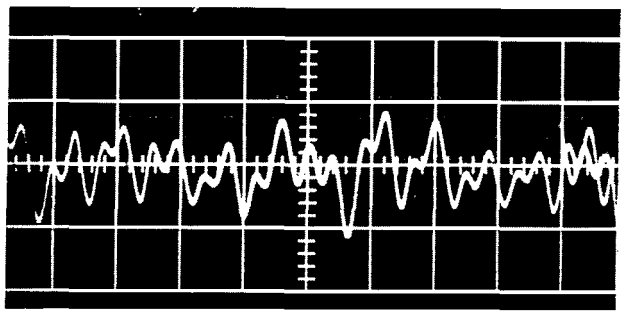

(a) 0 to 100 cps.

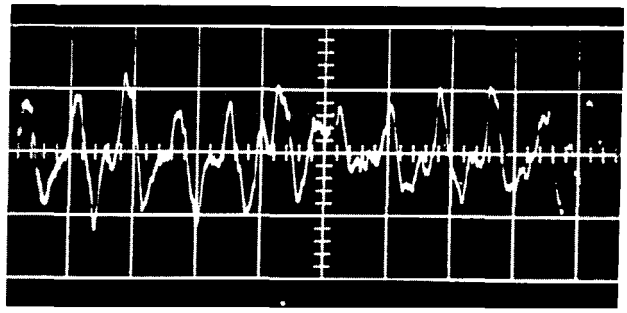

(b) 0 to 500 cps.

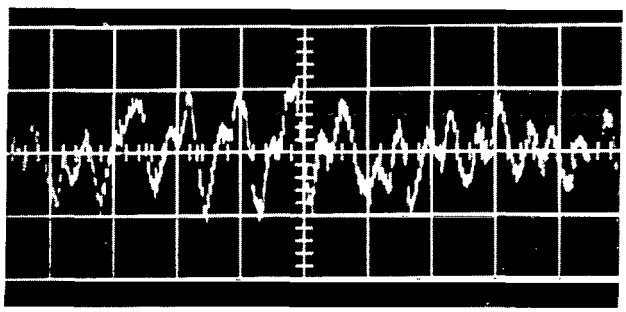

(c) 0 to 1000 cps.

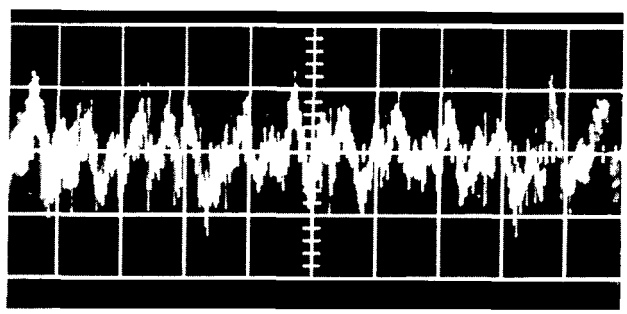

(d) 0 to 2000 cps.

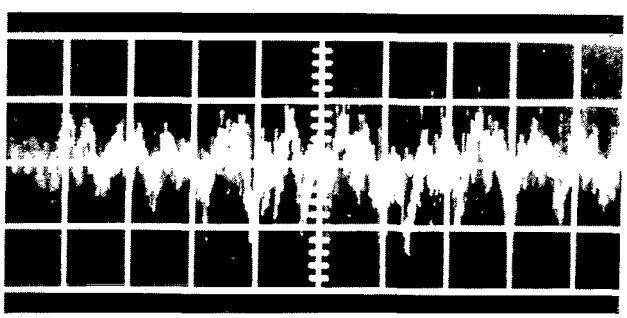

(e) 0 to 5000 cps.

Figure 14—Flutter traces; 20-millisec/cm sweep and 0.6 percent peak-to-peak flutter/cm.

Power measurements for satellite tape recorders are not always so easy to obtain or analyze as implied above because, along with all the testing done at room temperature, the recorder must be tested under various environmental conditions such as different humidities, temperature variations from 0° to 60°C, and different sinusoidal and random vibrations. All of these conditions, except the vibrations, will cause the power to change from that measured at ambient conditions just by being exposed to them. On the other hand, however, vibration will cause a change in power only when a component has been damaged severely enough to reflect a change (e.g., ball bearing damage).

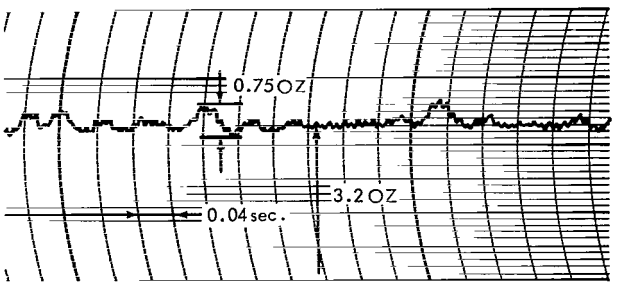

Figure 15—Tape tension trace.

Amplitude Measurements

The type of amplitude measurement taken is a trace of the envelope of the amplitude modulation of the reproduced signal. Tape transport irregularities (e.g., skew, dirt buildup on tape and heads, and vertical displacement of tape during a complete cycle) are reflected as a variation in amplitude of the playback signal. When this trace is properly analyzed it is very useful in locating periodic frequencies causing the disturbance.

As an example, Figure 16 is a trace of the amplitude modulation of a 50-kc signal recorded and played back at 33 ips. Its flutter traces appear in Figure 14. It is clearly seen that a frequency of approximately 117 cps is present. The calibration of the trace is:

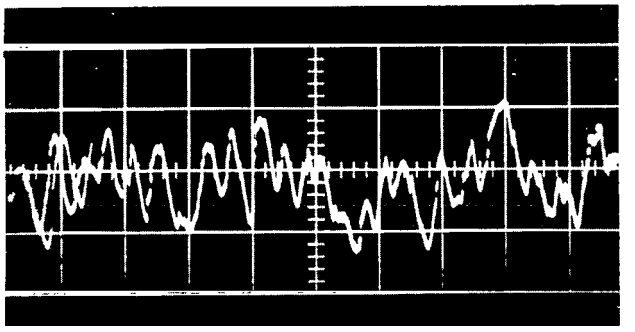

Figure 16—Amplitude modulation trace.

1. 20 millisec/cm sweep
2. 5 percent peak-to-peak AM/cm

CONCLUDING REMARKS

In the normal prototype and flight system programs the components are subjected to many days of environmental testing (e.g., vibrations, temperature and vacuum tests), both as a component and together with the flight system (associated electronics, housing, etc.). After the recorder and its system have successfully passed all the environmental testing they are integrated with the spacecraft and subjected to the spacecraft environmental tests.

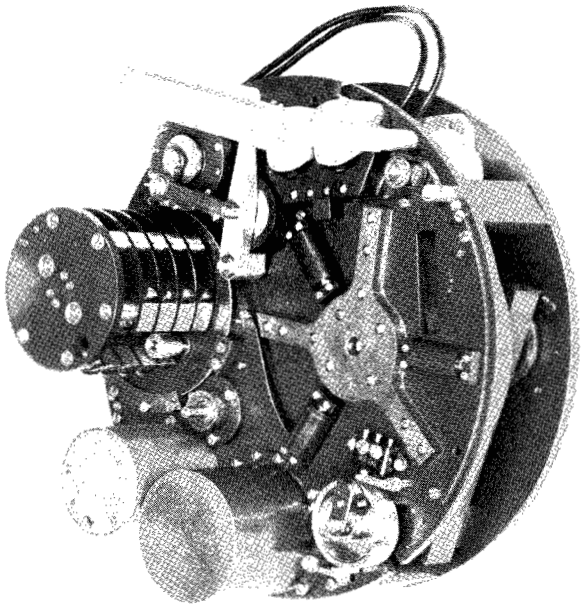

(a) 1/4-inch by 200-foot endless-loop transport developed for and flown on the Tiros program.

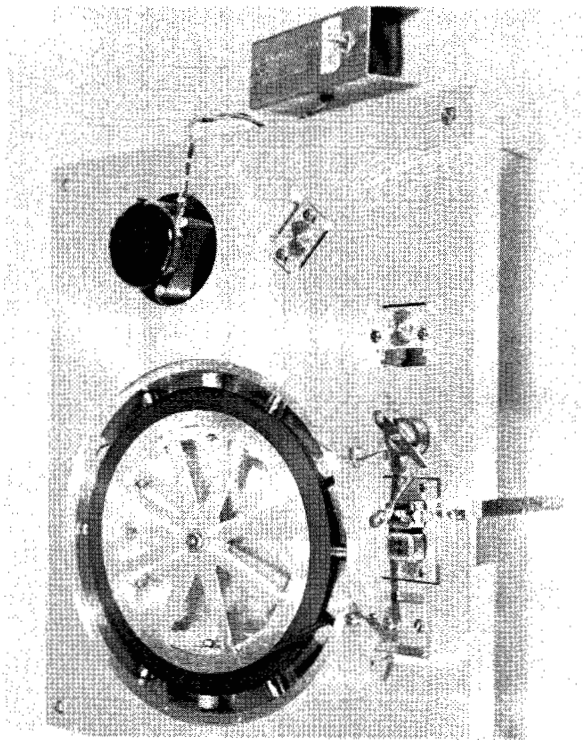

(b) 1/4-inch by 1200-foot test breadboard used for initial development work.

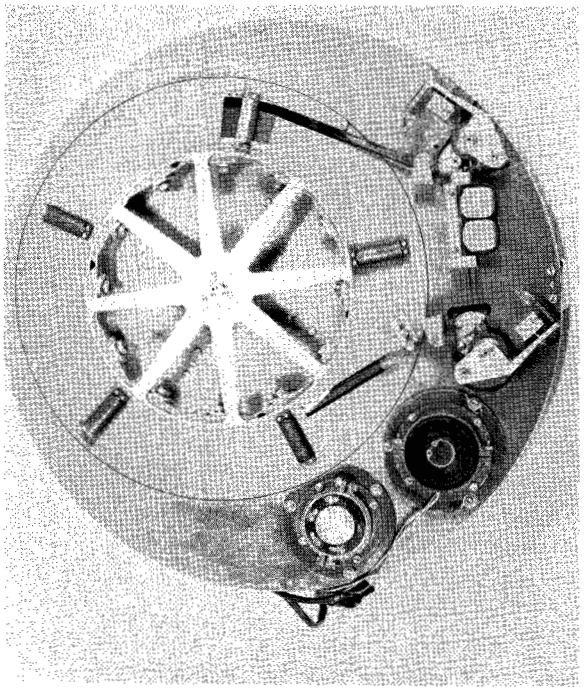

(c) 1/4-inch by 1200-foot preprototype model.

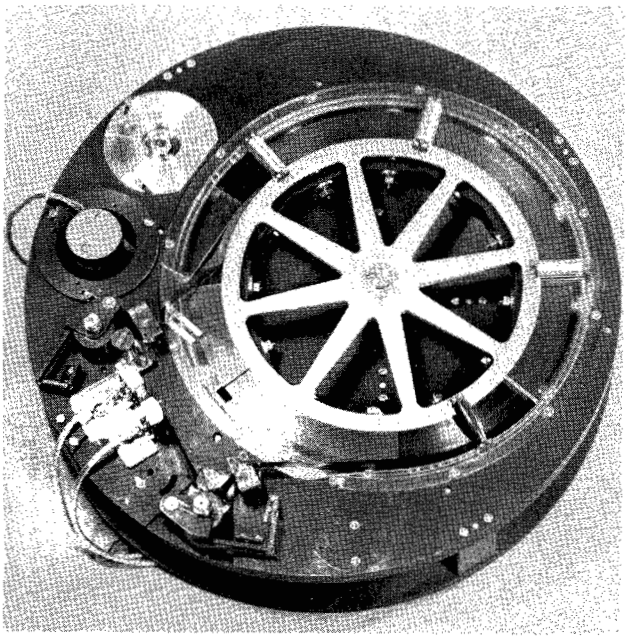

(d) 1/2-inch by 1200-foot preprototype model.

Figure 17—Endless-loop transports developed for the meteorological programs.

It is easily seen that a precision instrument such as a tape recorder cannot be haphazardly designed because a failure on the spacecraft during testing could cause large monetary losses because of the time lost during the extensive disassembly, testing and replacement of the component. Recorder failure would be even more serious if it resulted in a delay in the launch schedule or if it occurred while the spacecraft was in orbit and caused the loss of vital information or, possibly, the failure of the whole mission.

Photographs of endless-loop transports which were developed for the meteorological programs (References 7, 8, and 9) are given in Figure 17.

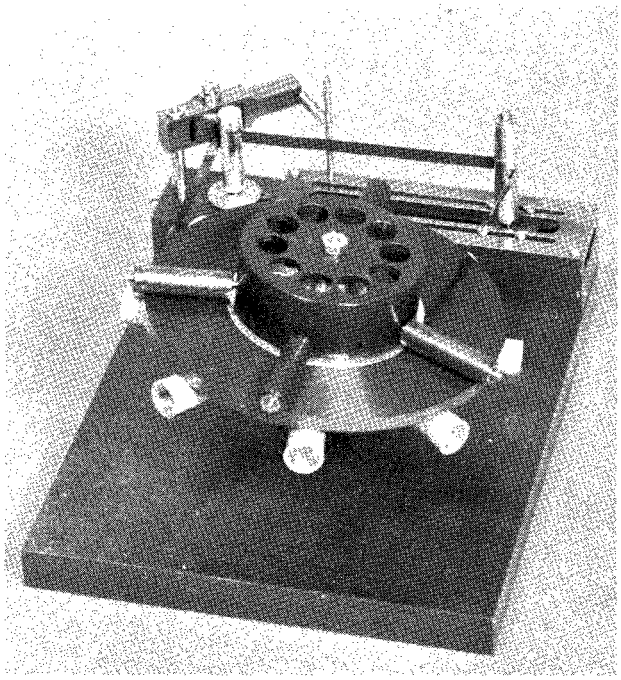

(e) 1/4-inch by 1200-foot compact test fixture.

Figure 17 cont.—Endless-loop transports developed for the meteorological programs.

ACKNOWLEDGMENT

The author is indebted to Dr. S. C. Ling, Professor, The Catholic University of America, for his advice and assistance.

(Manuscript received August 4, 1965)

REFERENCES

1. Roark, R. J., "Formulas for Stress and Strain," New York: McGraw Hill, 1954.
2. Bisson, E. E., and Anderson, W. J., "Advanced Bearing Technology," NASA Special Publication SP-38, 1964.
3. Licht, J., and White, A., "Polyester Film Belts," NASA Technical Note D-668, May 1961.
4. Thomson, W. T., "Mechanical Vibrations," 2d ed., Englewood Cliffs, N. J.: Prentice-Hall, 1953.
5. Stewart, W. E., "Magnetic Recording Techniques," New York: McGraw Hill, 1958.
6. Davies, G. L., "Magnetic Tape Instrumentation," New York: McGraw Hill, 1961.
7. Falwell, R. C., Stark, K. W., White, A. F., "A Precision Endless-Loop Magnetic Tape Recorder for Space Applications," NASA Technical Note D-1542, February 1963.
8. Stark, K. W., "Development of a 1200 Foot Endless-Loop Tape Transport for Satellite Applications," NASA Technical Note D-2316, June 1964.
9. Stark, K. W., and White, A. F., "Survey of Continuous-Loop Magnetic Tape Recorders Developed for Meteorological Satellites," NASA Technical Note D-2766, May 1965.
10. "A Theoretical and Practical Evaluation of the Dynamics of an Endless-Loop Tape Cartridge." Final Report NASA Contract NAS 5-2435. General Kinetics, Inc., Arlington, Virginia.

Appendix A

List of Symbols

A	Total contact area between layers of tape, sq. in.
A_1	Cross-sectional area of bearing outer race, sq. in.
A_2	Cross-sectional area of bearing spacer, sq. in.
a	Outer radius of bearing preload cap, in.
a_W	Outer radius of spring washer, in.
B	Bandwidth
b	Inner radius of bearing preload cap, in.
b_W	Inner radius of spring washer, in.
C	Point on bearing ball
C'	Point on bearing ball after rotating through angle θ
C_1, C_2	Belt damping constants
C_M	Torsional motor damping constant
D	Power spectral density
d_1	Diameter of tape cartridge reel, in.
d_2	Outer diameter of tape pack, in.
d_B	Bearing ball diameter
d_m	Mean tape pack diameter, in.
E	Modulus of elasticity, psi
E_1	Modulus of elasticity of bearing outer race, psi
E_2	Modulus of elasticity of bearing spacer, psi
E_3	Modulus of elasticity of preload cap, psi
F	Force as seen on pulley 1 at radius R_1 due to reflected torque from pulley 2
F'	$T_1 - T_2$
F_0	Tangential force at radius r_0, oz
F_1	Tangential force at radius R_1, oz
F_2	Tangential force at radius R_2, oz
F_3	Tangential force at radius r_1, oz

f_N	Natural frequency, cps
g	Gravitational constant
I	Inertia of tape pack
I_0, I_1, I_2	Pulley inertias
I_R	Inertia reflected back to motor
$K_{1,2}$	Equation constants
k	Spring constant, lb/in.
k_1, k_2	Belt spring constants
k_M	Torsional motor spring constant
k_T	Constant for given tape cartridge
L	Length of tape in cartridge, in.
L_1	Total width of outer bearing race, in.
ΔL_1	Compression of outer bearing race, in.
L_2	Half of outer bearing race spacer length, in.
ΔL_2	Compression of L_2, in.
L_3	Thickness of bearing preload cap, in.
ΔL_3	Deflection of bearing preload cap, in.
L_O	Operating tape loop length, in.
L_T	Total tape length, in.
M	Mass, lb-sec ^{2}/ft
m	Reciprocal of Poisson's ratio
N	Tape layer width, in
n	Interlayer surface from outermost to innermost (n = 1 is the outermost interlayer)
P	Total compressive load or preload, lb
P_W	Spring washer applied load, lb
P_P	Power required to drive tape pack, watts
R	Bearing radial load, lb
R_1, R_2	Large pulley radii, in.
R_n	Radial distance from center of rotation to centerline of tape layer n, in.
R_O	Mean outer layer radius of tape pack, in.
R_r	Radius of tape cartridge reel, in.
r	Radius of pulleys in general, in.

Δr	Radial runouts (TIR) of pulleys, in.
r_0, r_1	Small pulley radii, in.
r_C	Radius of capstan, in.
r_{CP}	Radius of capstan pulley, in.
r_i	Radius of bearing inner race, in.
r_m	Radius from axis of bearing to center of bearing ball, in.
r_{MP}	Radius of motor pulley, in.
r_O	Radius of outer bearing race, in.
S	Rotation arc of bearing ball on outer race, in.
S_1	Stress in bearing outer race, lb/sq. in.
S_2	Stress in spacer material, psi
S_3	Stress in preload cap, psi
T	Bearing thrust load, lb
T_1	Tape exit tension from pack, oz
T_2	Tape entrance tension to pack, oz
T_e	Kinetic energy
t	Time, sec
t_P	Tape pack thickness, in.
t_W	Spring washer thickness, in.
t_T	Tape thickness, in.
V	Instantaneous velocity of point on bearing ball, in./sec
V_0	Velocity of pulley 0 at r_0
V_1	Velocity of pulley 1 at R_1
V_2	Velocity of pulley 2 at R_2
V_b	Velocity of belt, in/sec.
V_C	Velocity of tape at capstan, in./sec
V_m	Velocity of bearing ball center, in./sec
v_1	Velocity of pulley 1 at r_1
W	Weight of assembly multiplied by 20 g's, lb
Y_{max}	Maximum deflection of spring washer, in.
α	Angle ball makes with bearing axis when rotating through arc S, rad
β	Bearing contact angle
δ	Initial bearing outer race stickout, in.

δ_B	Bearing deflection under loading, taken from load-deflection curves, in.
ϵ	Strain, in./in.
θ	Rotation angle of bearing ball, rad
$\theta_0, \theta_1, \theta_2$	Pulley displacements with respect to θ_0', θ_1', θ_2'
$\theta_0', \theta_1', \theta_2'$	Noncompliant pulley displacements
$\lambda_{1,2}$	Damping rates of $K_{1,2}$
ρ	Tape density, lb/in.^{3}
σ	Standard Gaussian deviation
$\tau(t)$	Motor driving torque as a function of time, in.-oz
τ_R	Total reflected torque at first pulley, in.-oz
$\tau_0', \tau_1', \tau_2'$	Torques of respective pulleys as seen at first pulley, in.-oz
$\phi_{1,2}$	$= \sqrt{-M_9}$
ω_B	Frequency of point C on bearing ball, θ/t
ω_B'	Frequency caused by point on bearing ball hitting inner and outer races
ω_C	Angular rotation of capstan, rad/sec
ω_i	Inner bearing race frequency
ω_M	Angular rotation of motor, rad/sec
ω_{MP}	Angular rotation of motor pulley, rad/sec
ω_m	Ball frequency about axis of bearing, rad/sec, α/t
ω_N	Resonant rate, rad/sec
ω_n	Angular velocity of tape layer n, rad/sec
$\Delta\omega_n$	Interlayer angular velocity difference at tape layer n
$(\omega_{n+1} - \omega_n)$	Angular velocity difference between two successive tape layers
ω_O	Outer bearing race frequency, rad/sec
$\omega_{1,2}$	Rotating frequencies of $K_{1,2}$
$(\dot{})$ $(\ddot{})$	First and second derivatives with respect to time

Appendix B

Endless-Loop Cartridge Operation

The 1/4-inch by 1200-foot endless-loop tape transport shown in Figure B1 will be utilized to explain the operation of endless-loop tape cartridges in general. The tape is first wrapped onto reel (a) and rollers (b) by starting the first wrap at the edge of the reel and the tapered portion of the rollers. Successive wraps are built up progressively toward the edge of the rollers until 1200 feet have been used. The two ends of the tape are brought up through tape guide plate (c) and are spliced to form an endless loop. When the cartridge is in operation, the tape is pulled from the first wrap on the reel by the capstans (d) and it wraps back onto the outside of the tape pack. As the tape moves at constant velocity, each layer of tape slips upon the next layer, thus providing tension to pull the tape back down into the cartridge on the return side (e).

Note that uniform slippage of each layer of tape in the cartridge is important if optimum performance of the recorder is to be obtained. As the tape becomes worn and the lubrication deteriorates the layers start to stick and slippage no longer is uniform. If the tape is not changed and the cartridge is allowed to operate beyond this point, the cartridge will have a non-slip failure.

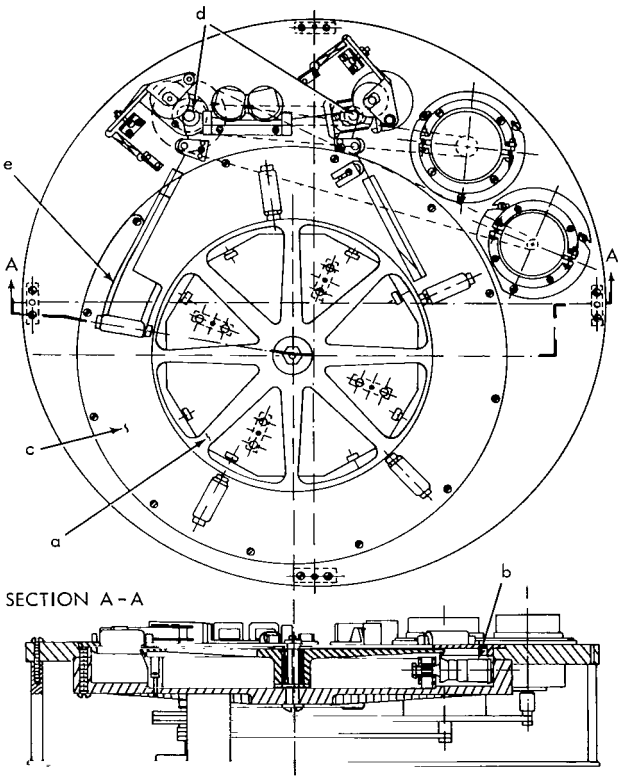

Figure B1—The 1200-foot endless-loop tape transport assembly.

Appendix C

Increase in Interlayer Angular Velocity Difference Due to Decreased Mean Tape Pack Diameters for Constant Tape Length Systems

The following derivation determines the interlayer angular velocity difference for the tape pack shown in Figure 7. Here $V_C = R_n \omega_n$ or $\omega_n = V_C/R_n$.

The angular velocity difference between two successive layers of tape is

$$(\omega_{n+1} - \omega_n) = \frac{V_C}{(R_n - t_T)} - \frac{V_C}{R_n} = V_C \left[\frac{t_T}{R_n (R_n - t_T)}\right].$$

The angular velocity difference at the nth interlayer can be expressed as

$$\Delta\omega_n = \frac{V_C\, t_T}{R_0 (R_0 - 2t_T n + t_T) + t_T^2\, n(n-1)}. \quad \text{(C1)}$$

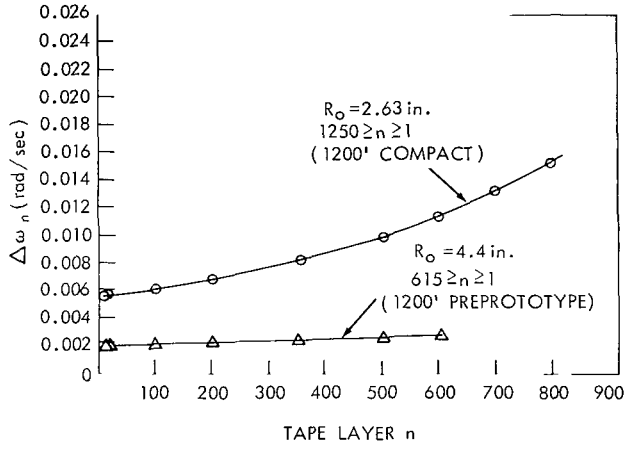

Figure C1—Interlayer angular velocity difference $\Delta\omega_n$ (Equation C1) against tape layer n. Tape velocity, 30 ips; tape thickness, 0.0013 inch; R_0, mean outer layer radius of tape pack, inch.

This equation is plotted in Figure C1 for two tape cartridges, each containing 1200 feet of 1/4-inch magnetic tape. The compact cartridge has a smaller mean pack diameter than does the preprototype; R_0 = 2.63 inch for the compact recorder and R_0 = 4.4 inch for the preprototype recorder.

From the curves it is seen that the average $\Delta\omega_n$ is larger for the compact recorder than for the preprototype. As was discussed in this report the total interlayer contact area of the tape cartridge does not change significantly, for large lengths of tape, when tape cartridges of various mean diameters and constant tape lengths are built. Therefore, the tape wear and frictional drag within the cartridge increases for the compact version.

From a design standpoint, where total operating lifetime and power are important, it is best to utilize a cartridge design with a mean diameter d_m as large as practicable.

"The aeronautical and space activities of the United States shall be conducted so as to contribute . . . to the expansion of human knowledge of phenomena in the atmosphere and space. The Administration shall provide for the widest practicable and appropriate dissemination of information concerning its activities and the results thereof."

—NATIONAL AERONAUTICS AND SPACE ACT OF 1958

NASA SCIENTIFIC AND TECHNICAL PUBLICATIONS

TECHNICAL REPORTS: Scientific and technical information considered important, complete, and a lasting contribution to existing knowledge.

TECHNICAL NOTES: Information less broad in scope but nevertheless of importance as a contribution to existing knowledge.

TECHNICAL MEMORANDUMS: Information receiving limited distribution because of preliminary data, security classification, or other reasons.

CONTRACTOR REPORTS: Technical information generated in connection with a NASA contract or grant and released under NASA auspices.

TECHNICAL TRANSLATIONS: Information published in a foreign language considered to merit NASA distribution in English.

TECHNICAL REPRINTS: Information derived from NASA activities and initially published in the form of journal articles.

SPECIAL PUBLICATIONS: Information derived from or of value to NASA activities but not necessarily reporting the results of individual NASA-programmed scientific efforts. Publications include conference proceedings, monographs, data compilations, handbooks, sourcebooks, and special bibliographies.

Details on the availability of these publications may be obtained from:

SCIENTIFIC AND TECHNICAL INFORMATION DIVISION

NATIONAL AERONAUTICS AND SPACE ADMINISTRATION

Washington, D.C. 20546